Physical plasma therapy accelerates wound re-epithelialisation and enhances extracellular matrix formation in cutaneous skin grafts

Nadira Frescaline, Constance Duchesne, Maryline Favier, Rachel Onifarasoaniaina, Thomas Guilbert, Georges Uzan, Sébastien Banzet, A. Rousseau, Jean-jacques Lataillade

▶ **To cite this version:**

Nadira Frescaline, Constance Duchesne, Maryline Favier, Rachel Onifarasoaniaina, Thomas Guilbert, et al.. Physical plasma therapy accelerates wound re-epithelialisation and enhances extracellular matrix formation in cutaneous skin grafts. Journal of Pathology, 2020, 252 (4), pp.451-464. 10.1002/path.5546 . hal-02986638

HAL Id: hal-02986638

https://hal.sorbonne-universite.fr/hal-02986638

Submitted on 3 Nov 2020

HAL is a multi-disciplinary open access archive for the deposit and dissemination of scientific research documents, whether they are published or not. The documents may come from teaching and research institutions in France or abroad, or from public or private research centers.

L'archive ouverte pluridisciplinaire **HAL**, est destinée au dépôt et à la diffusion de documents scientifiques de niveau recherche, publiés ou non, émanant des établissements d'enseignement et de recherche français ou étrangers, des laboratoires publics ou privés.

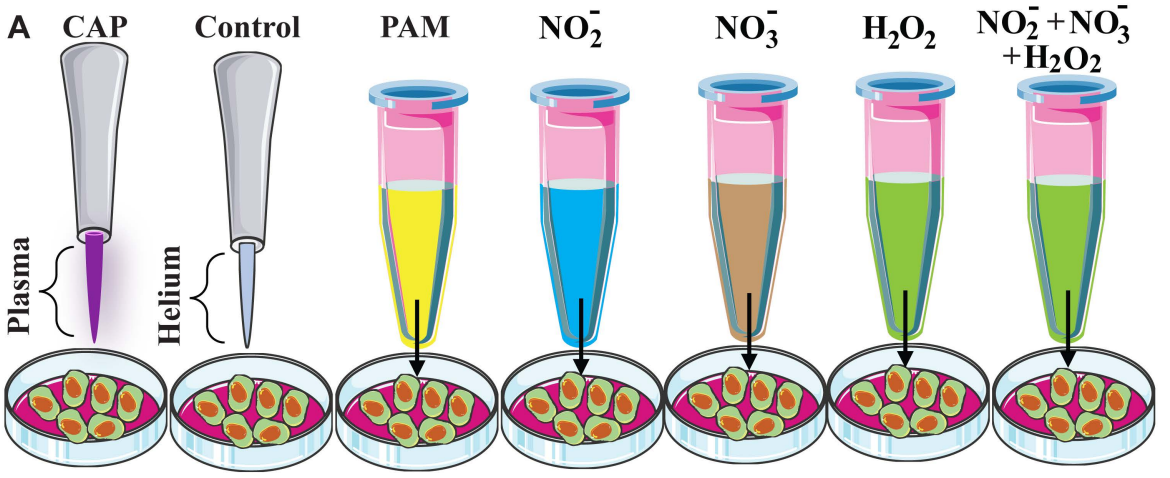
A
CAP
Control
PAM
NO_2^-
NO_3^-
H_2O_2
$NO_2^- + NO_3^- + H_2O_2$
Plasma
Helium

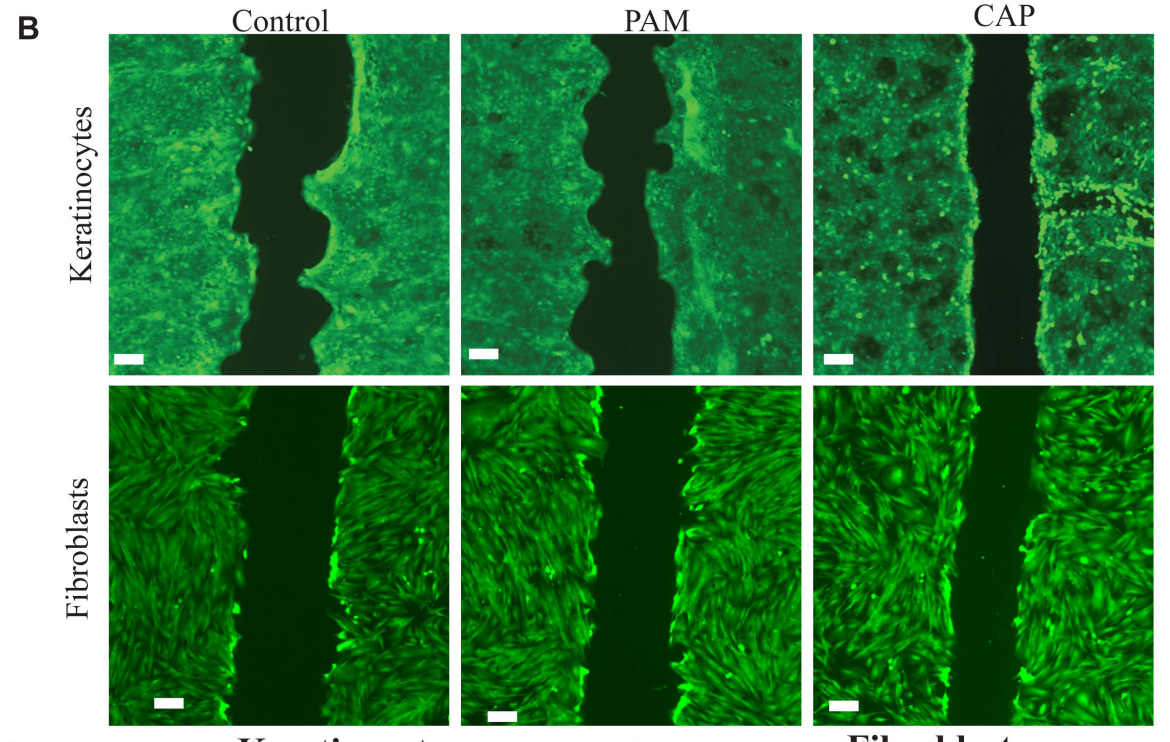
B
Control
PAM
CAP
Keratinocytes
Fibroblasts

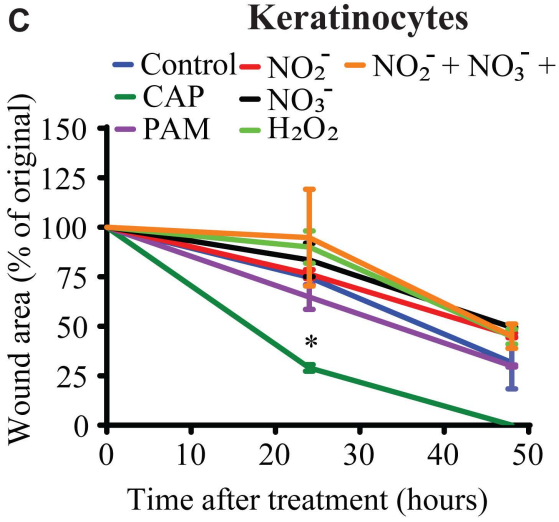
C
Keratinocytes
Control
NO_2^-
$NO_2^- + NO_3^- + H_2O_2$
CAP
NO_3^-
PAM
H_2O_2
Wound area (% of original)
150
125
100
75
50
25
0
0
10
20
30
40
50
Time after treatment (hours)
*

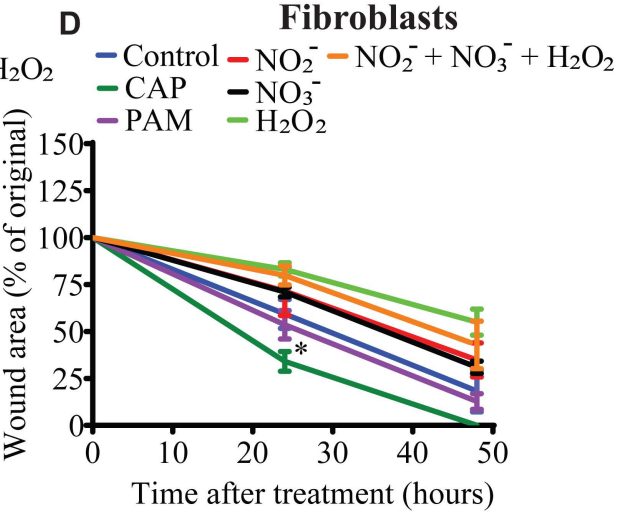
D
Fibroblasts
Control
NO_2^-
$NO_2^- + NO_3^- + H_2O_2$
CAP
NO_3^-
PAM
H_2O_2
Wound area (% of original)
150
125
100
75
50
25
0
0
10
20
30
40
50
Time after treatment (hours)
*

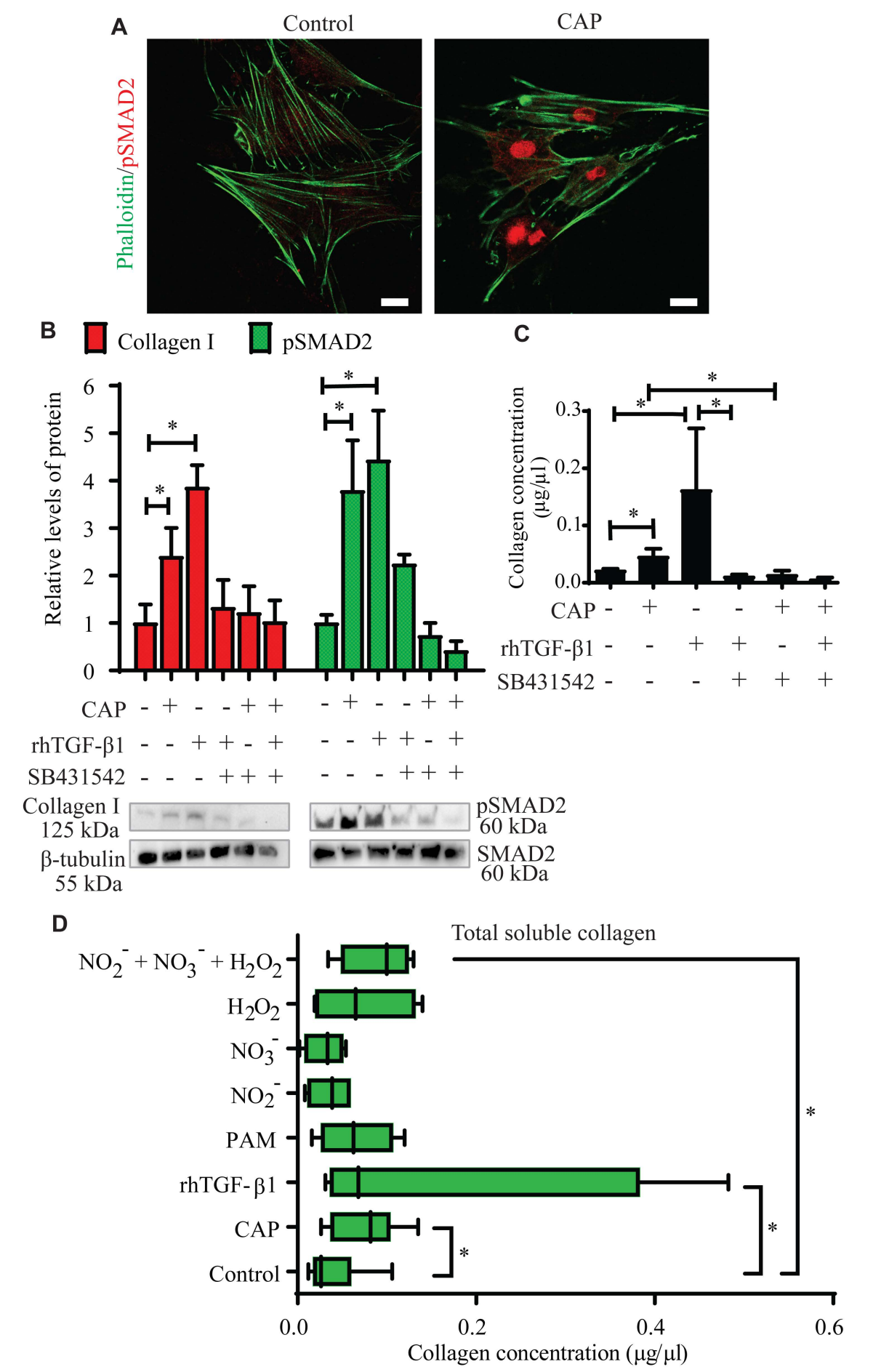
A
Control
CAP
Phalloidin/pSMAD2
B
Collagen I
pSMAD2
Relative levels of protein
CAP
rhTGF-β1
SB431542
Collagen I
125 kDa
β-tubulin
55 kDa
pSMAD2
60 kDa
SMAD2
60 kDa
C
Collagen concentration (μg/μl)
CAP
rhTGF-β1
SB431542
D
Total soluble collagen
$NO_2^- + NO_3^- + H_2O_2$
H_2O_2
NO_3^-
NO_2^-
PAM
rhTGF-β1
CAP
Control
Collagen concentration (μg/μl)

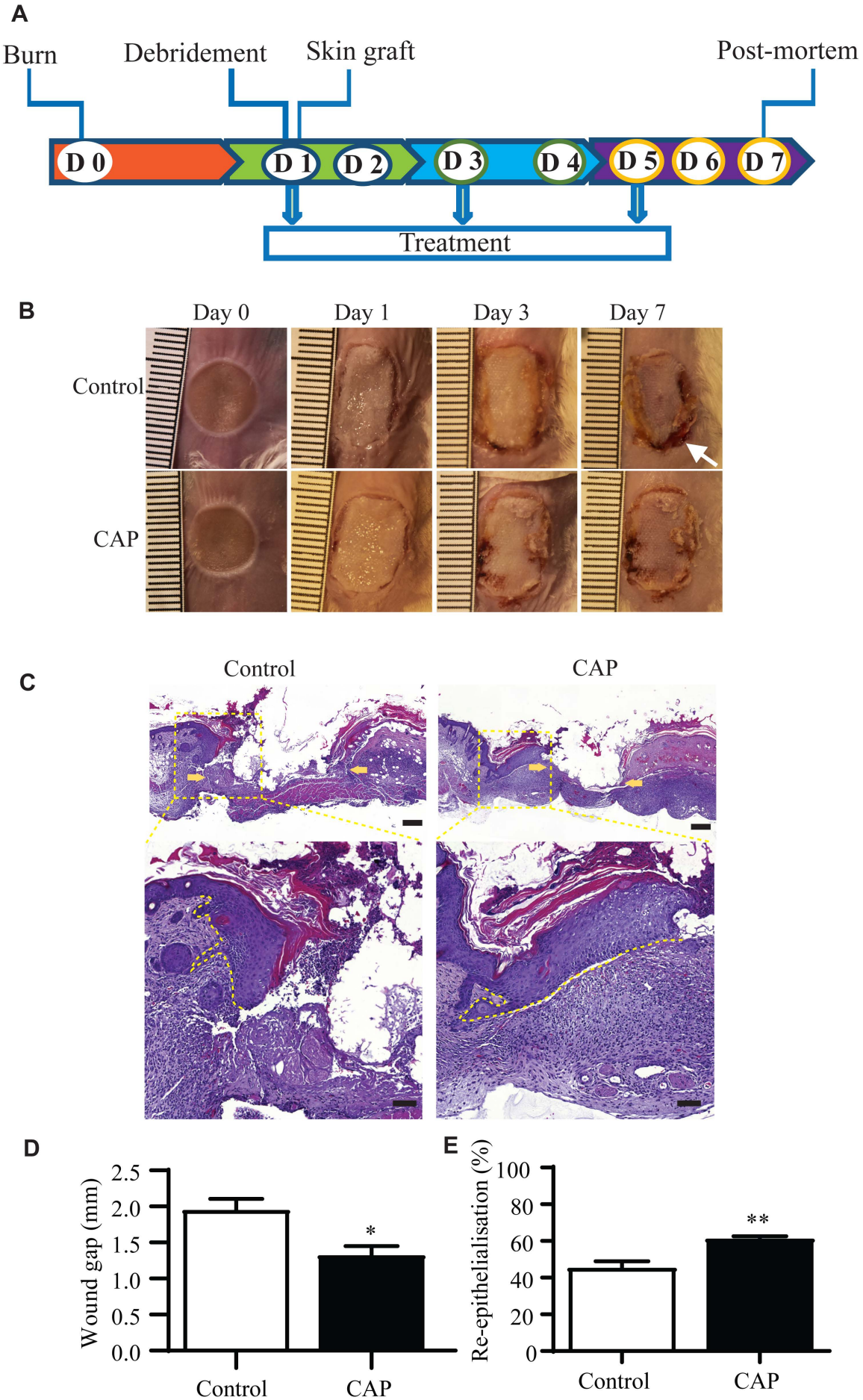
A
Burn
Debridement
Skin graft
Post-mortem
D 0
D 1
D 2
D 3
D 4
D 5
D 6
D 7
Treatment
B
Day 0
Day 1
Day 3
Day 7
Control
CAP
C
Control
CAP
D
Wound gap (mm)
2.5
2.0
1.5
1.0
0.5
0.0
*
Control
CAP
E
Re-epithelialisation (%)
100
80
60
40
20
0
**
Control
CAP

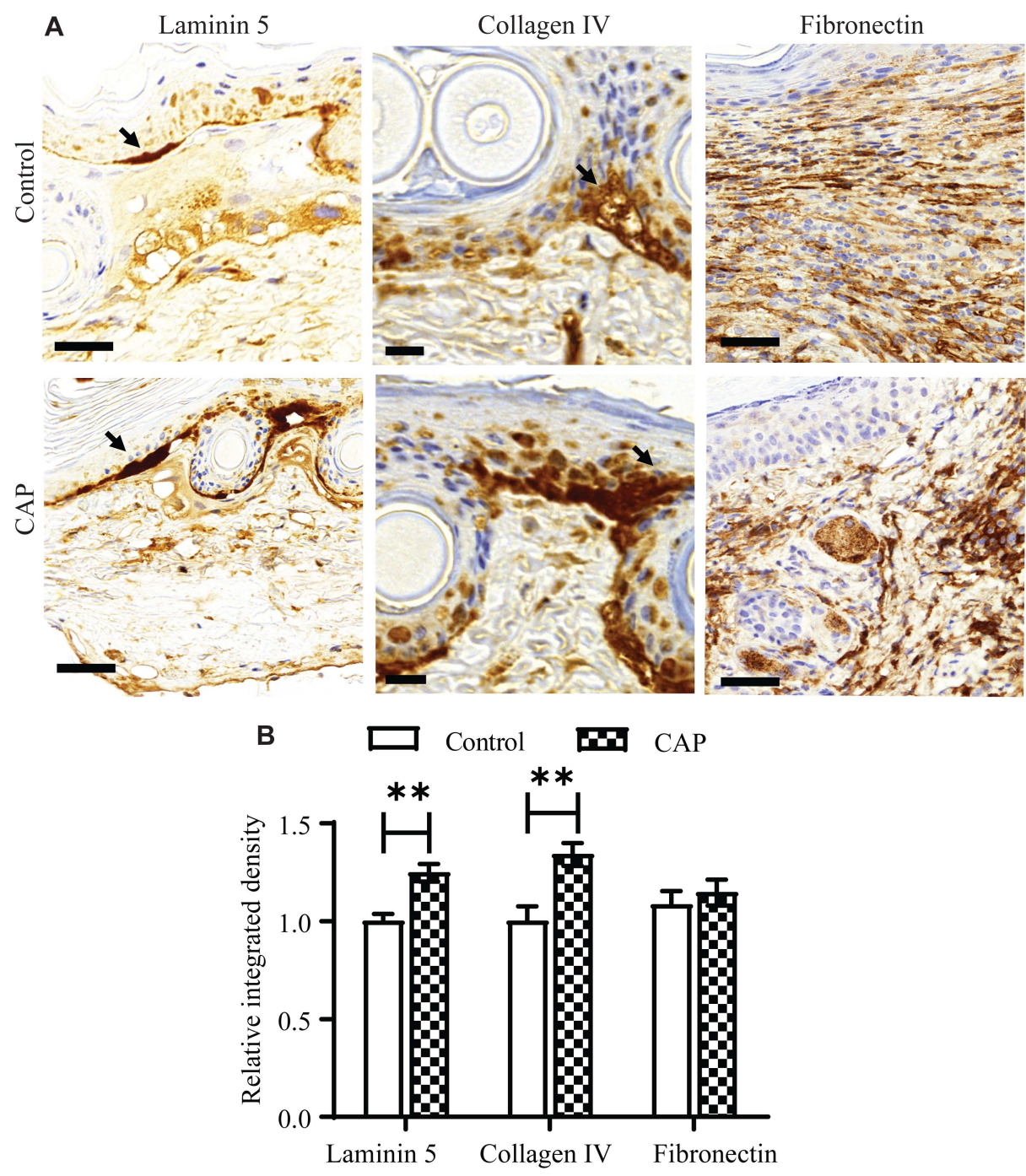
A
Laminin 5
Collagen IV
Fibronectin
Control
CAP
B
Control
CAP
**
**
Relative integrated density
1.5
1.0
0.5
0.0
Laminin 5
Collagen IV
Fibronectin

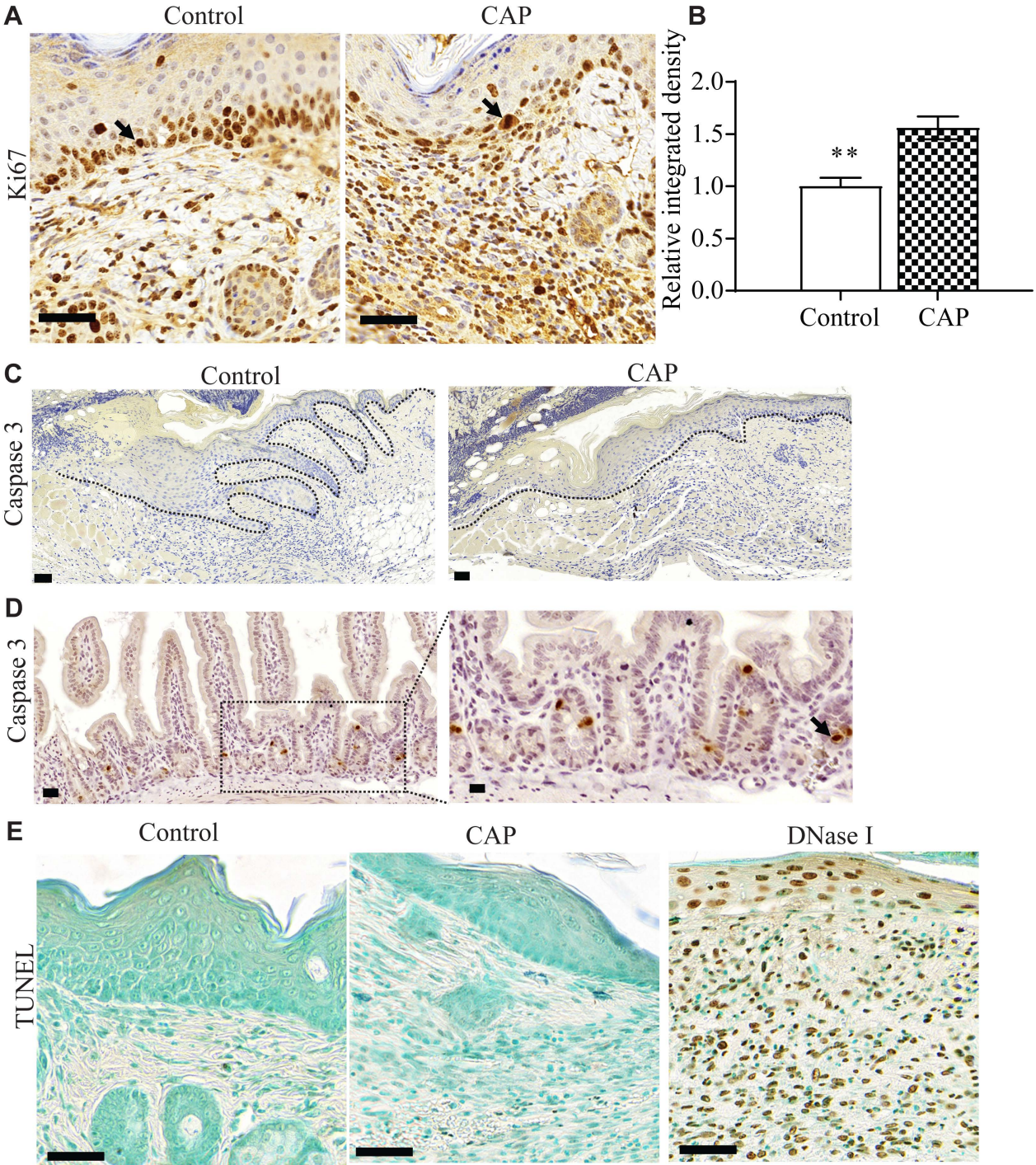
A
Control
CAP
Ki67
B
Relative integrated density
2.0
1.5
1.0
0.5
0.0
**
Control
CAP
C
Control
CAP
Caspase 3
D
Caspase 3
E
Control
CAP
DNase I
TUNEL

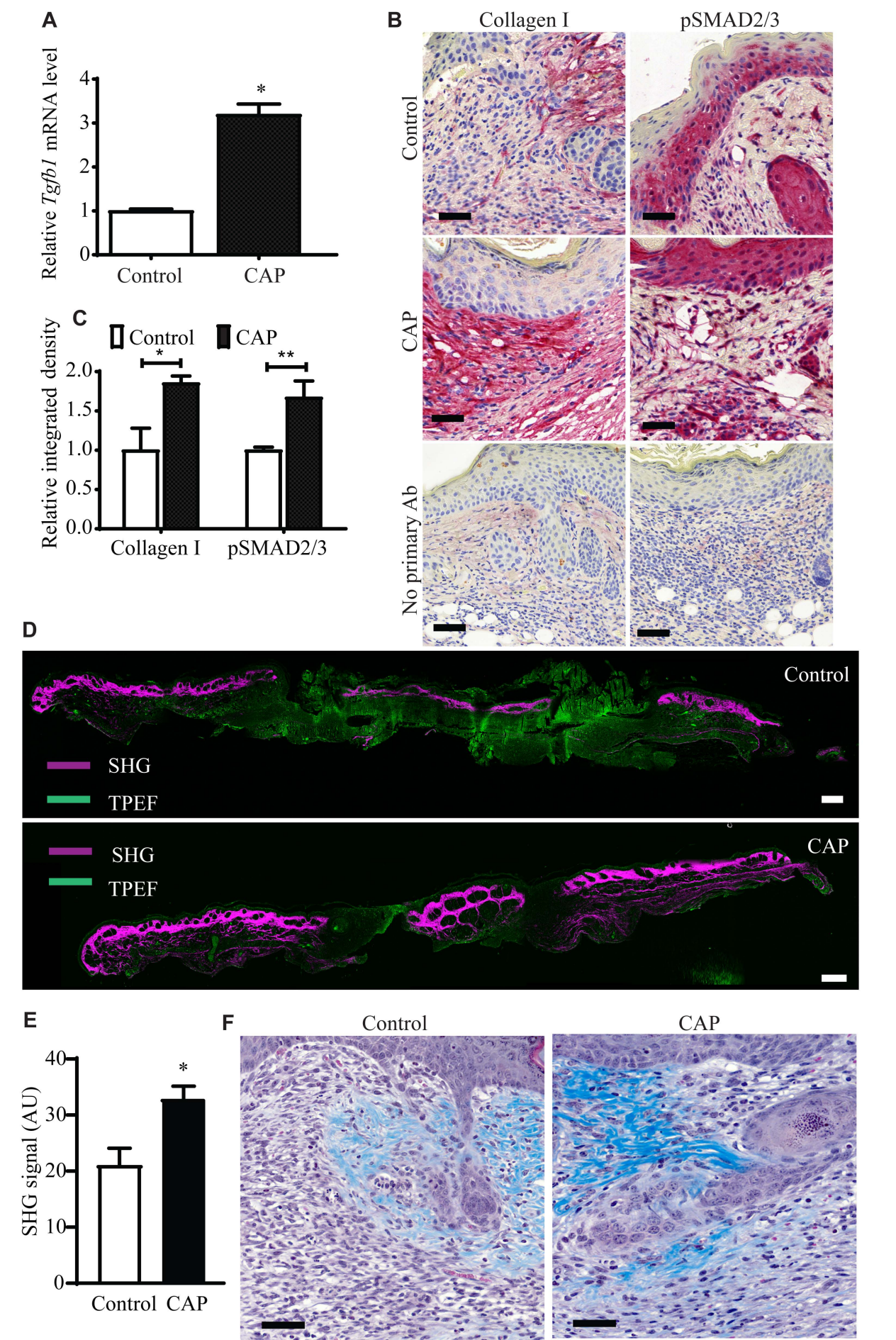
A
Relative Tgfb1 mRNA level
4
3
2
1
0
*
Control
CAP
B
Collagen I
pSMAD2/3
Control
CAP
No primary Ab
C
Control
CAP
Relative integrated density
2.0
1.5
1.0
0.5
0.0
*
**
Collagen I
pSMAD2/3
D
Control
SHG
TPEF
SHG
TPEF
CAP
E
SHG signal (AU)
40
30
20
10
0
*
Control
CAP
F
Control
CAP

Title: Physical plasma therapy accelerates wound re-epithelialisation and enhances extracellular matrix formation in cutaneous skin grafts

Short running title: Cold atmospheric plasma improves burn repair and skin graft integration

Authors: Nadira Frescaline[1,2*], Constance Duchesne[1,2*], Maryline Favier[3], Rachel Onifarasoaniaina[3], Thomas Guilbert[3], Georges Uzan[4], Sébastien Banzet[1], Antoine Rousseau[2], Jean-Jacques Lataillade[1]

Affiliations:

[1] INSERM UMRS-MD 1197, Institut de Recherche Biomédicale des Armées, Centre de Transfusion sanguine des Armées, 92141 Clamart, France

[2] Laboratoire de physique des plasmas, École Polytechnique, Sorbonne Université, Université Paris Saclay, CNRS, 91128 Palaiseau, France

[3] Institut Cochin, INSERM U1016, CNRS UMR8104, Université de Paris, F-75014 Paris, France

[4] INSERM UMRS-MD 1197, Hôpital Paul Brousse, Villejuif, France

***Note:** Nadira Frescaline and Constance Duchesne contributed equally to this article.

Corresponding author: Dr Nadira Frescaline

Address: Institut de Recherche Biomédicale des Armées, INSERM UMRS-MD 1197, Centre de Transfusion sanguine des Armées, 92141 Clamart, France

Email: nadira.frescaline@lpp.polytechnique.fr

Telephone: +33 1 69 33 58 78

Keywords: full-thickness burn wound, cold atmospheric plasma, collagen, wound healing, SMAD, TGF-β, extracellular matrix, dermal-epidermal junction

Abstract

Skin grafting is a surgical method of cutaneous reconstruction, which provides volumetric replacement in wounds unable to heal by primary intention. Clinically, full-thickness skin grafts (FTSG) are placed in aesthetically sensitive and mechanically demanding areas such as the hands, face and neck. Complete or partial graft failure is the primary complication associated with this surgical procedure. Strategies aimed at improving the rate of skin graft integration will reduce the incidence of graft failure.

Cold atmospheric plasma (CAP) is an emerging technology offering innovative clinical applications. This study is aimed to test the therapeutic potential of CAP to improve wound healing and skin graft integration into the recipient site. *In vitro* models that mimic wound healing were used to investigate the ability of CAP to enhance cellular migration, a key factor in cutaneous tissue repair. We demonstrate that CAP enhances the migration of epidermal keratinocytes and dermal fibroblasts. This increased cellular migration was possibly induced by the low dose of reactive oxygen and nitrogen species produced by CAP. Using a murine model of burn wound reconstructed with a full-thickness skin graft, we show that wounds treated with CAP healed faster than did control wounds. Immunohistochemical wound analysis showed that CAP treatment enhanced the expression of the dermal-epidermal junction components, which are vital for successful skin graft integration. CAP treatment was characterised by increased levels of *Tgfbr1* mRNA and collagen I protein *in vivo*, suggesting enhanced wound maturity and extracellular matrix deposition. Mechanistically, we show that CAP induced the activation of the canonical SMAD-dependent TGF-β1 pathway in primary human dermal fibroblasts, which may explain the increased collagen I synthesis *in vitro*. These studies reveal that CAP improves wound repair and

skin graft integration via mechanisms involving extracellular matrix formation. CAP offers a novel approach for treating cutaneous wounds and skin grafts.

INTRODUCTION

Skin grafting is the transfer of cutaneous tissue from a donor site to another anatomical location. This surgical technique is frequently necessary to repair skin lesions resulting from burn injury, tumour resection, chronic wounds and other pathological conditions [1,2]. Full-thickness skin grafts (FTSGs) are common choices when it comes to reconstructing smaller wounds over mechanically demanding areas of the body such as the joints [3,4]. FTSGs are associated with a lower incidence of contractures [5], result in a more aesthetical outcome [1,3] and, therefore, deemed suitable for wounds on exposed areas of the body [1,4]. The main complication seen with FTSGs is related to complete or partial graft failure [6]. Early graft failure is attributed to several factors including inadequate formation of anastomoses between the recipient site and donor skin [6,7]. We recently demonstrated that treatment with physical plasma leads to improved wound angiogenesis and skin graft vascularization [8]. In addition to efficient angiogenesis, successful skin graft integration is very likely to be dependent on wound re-epithelialisation. Wound re-epithelialisation is achieved by a combination of proliferation and migration of epidermal keratinocytes that crawl collectively as a cellular sheet [9]. During re-epithelialisation migrating keratinocytes [10] and dermal fibroblasts synthesise basement membrane (BM) proteins, which make up the dermal-epidermal junction (DEJ) - structure that tightly binds the epidermis to the dermis [11]. Skin fibroblasts are the major mesenchymal cell type in cutaneous tissue known to be involved in DEJ-BM restoration after injury. Dermal fibroblast deposit collagen and elastic fibres of the extracellular matrix (ECM) – bioactive structure with diverse roles in mechanical

support, activation of growth factors and cell anchorage [12]. As the donor graft is slowly degraded it becomes replaced by fibroblasts capable of producing the DEJ-BM and ECM. Fibroblasts are drawn from the healthy dermis of the recipient wound bed margins into the donor graft that provides a scaffold system where these cells can proliferate and synthesis new ECM. Numerous molecular pathways can contribute to the production of collagen-rich ECM by dermal fibroblasts, but two key mechanisms known to stimulate ECM synthesis are transforming growth factor-β (TGF-β)/SMAD-dependent and TGF-β/SMAD-independent pathways [13,14]. Activation of TGF-β1 induces the expression of the genes encoding collagen I and collagen III in dermal fibroblasts [14]. In the early phase of the wound healing process, activation of TGF-β1 promotes wound closure via stimulation of new ECM formation and secretion of collagen I and fibronectin - proteins that facilitate re-epithelialisation [15] and strengthen the wound [7]. TGF-β1 acts through a pathway dependent on phosphorylation of intracellular SMAD2 and SMAD3 proteins by the TGF-β receptor 1 (TGFR1) [13].

Physical plasma is a partially ionised gas [16]. Plasma-generating devices emit a jet of plasma, which combines with the surrounding air and creates a large number of reduction/oxidation (redox)-based molecules, notably reactive oxygen and nitrogen species (RONS), such as chemically relatively stable hydrogen peroxide (H_2O_2), nitrite (NO_2^-), nitrate (NO_3^-) [16]. RONS act as signalling molecules, which maintain physiological functions and crucial mechanisms of homeostatic regulation. H_2O_2 is an example of a naturally produced and chemically relatively stable ROS that can diffuse in tissues and cross cell membranes. In wounds, H_2O_2 is produced at the margin and acts as an immune cell attractant that triggers these cells to migrate toward the injury within minutes after wounding [17,18].

Phase II randomized controlled trials tested the performance [19,20] and safety [21] of CAP on cutaneous wounds. These trials demonstrated clinical efficacy, however mechanisms through which the physicochemical signals elicited by CAP are transmitted to biological systems remain poorly understood. When it comes to tissue repair, clinical studies are limited by wide variability in factors such as anatomical location, initial size of wounds and genetic variation in the patient population. Animal studies, on the other hand, provide the ability to control several important variables. Mouse models of wound repair are associated with numerous advantages and limitations. The limitations are mostly related to the fact that mouse wounds heal by contraction [22]. No single preclinical model is able to recapitulate the totality of human wound repair. In this study, we suggest an *in vivo* mouse model of cutaneous tissue repair, which was used as a tool for elucidating possible cellular and molecular mechanisms activated by physical plasma. The aim of this study was to test the influence of physical plasma on cellular migration, formation of the DEJ and ECM. We hypothesized that CAP enhances DEJ restoration and ECM remodelling through efficient migration of cells from the recipient bed into the donor graft where they synthesise collagen-rich provisional matrix. To our knowledge, no one has studied the molecular pathways which may be triggered by CAP-generated RONS to produce new ECM and enhance collagen deposition in skin grafts. To address lack of knowledge, we investigated the influence of CAP on activation of signalling pathways which may favour the restoration of the DEJ-BM and ECM after burn injury and skin grafting in mice.

MATERIALS AND METHODS

Detailed methods are discussed in the Supplementary Materials and Methods.

Mouse burn injury and skin graft technique

All experimental procedures involving animals were conducted in accordance with institutional procedures and approved by relevant committee for animal experiments (Ministère de l'Enseignement Supérieur et de la Recherche; Ethics permit number: 201711161651767 0v2). Mouse burn injury studies were performed using 6 week-old female mice from the BALB⁄c background weighing 19–22 g (Janvier Labs, Saint Berthevin, France). Anaesthesia was induced as previously described [8]. A full-thickness burn wound was created as previously described [8]. Briefly, a single burn wound was induced on the back of the mouse using a pre-heated brass template. Twenty-four hours after the injury, burned tissue was surgically excised with scissors to the muscular fascia. Skin grafts were harvested from the tail of a donor BALB⁄c mouse, and fixed in place as previously described [8]. An inert paraffin gauze dressing (Adaptic, Systagenix, North Yorkshire, UK) and Micropore™ Surgical Tape (3M, Cergy-Pontoise, France) were applied. Reconstructed wounds were treated with CAP every second day (30 seconds) and harvested one week after the burn injury. For further details regarding the mouse studies, see the Supplementary Materials and Methods.

Microscopy and histological wound assessment

Mouse skin was fixed in 4% paraformaldehyde and embedded into paraffin. Sections of 4 μm were subjected to immunohistochemistry according to manufacturer's protocol (Leica Biosystems, Nanterre, France) and imaged using the Lamina automated microscope (Perkin Elmer, Waltham, MA, USA). A total of six microscopic fields of view were used for the immunohistochemical data analysis. Out of the six microscopic images, two represented the region around the left border of

the burn lesion, two additional images included the graft region and the two remaining images included the area around the right border of the burn wound. Both the epidermal and dermal regions were assessed, including the migrating tongue of the epidermis at the wound edge and within the dermal wound bed. Immunohistochemical staining was quantified as described previously [23,24]. Slides stained with haematoxylin and eosin were used to evaluate the microscopic dermal wound gape. ImageJ software was used to determine the length of the microscopic dermal wound gape by drawing a straight line between the dermal wound margins. To estimate the degree of re-epithelialisation (% of the original wound), the area of the wound that was covered with neo-epidermis was expressed as a percentage of the entire wound, as described previously [25,26]. Histological samples were randomised using a computer-based random number generator. Histological slide assessment and data acquisition were performed by two assessors. Only one of the two assessors was formally blinded.

STATISTICAL ANALYSIS

Data are expressed as mean ± standard error of the mean (SEM) and indicated in figures as $*p < 0.05$, $**p < 0.01$, $***p < 0.001$. Statistical analysis was performed as described previously [8] with GraphPad Prism version 8 (GraphPad Software, San Diego, California, USA). For a two-group comparison, a Student's t test was used, provided the pre-test for normality (D'Agostino-Pearson normality test) was not rejected at the 0.05 significance level; otherwise, a non-parametric Mann–Whitney U test was used. Details of statistical tests used, the n numbers for each experiment can be found in the figure legends.

RESULTS

The dose-dependent effect of CAP on the concentration of RONS in plasma-activated medium *in vitro*

A plasma jet was designed and assembled. The plasma jet and its gaseous discharge were used to treat cellular monolayers *in vitro* and mouse skin *in vivo* (supplementary material, Figure S1A-B). The plasma jet was characterised by a violet-tinted stream of gas (supplementary material, Figure S1C). The RONS produced by the gaseous discharge at the gas-liquid interface [27] were previously described to induce various biological reactions including increased cellular migration and proliferation [28,29]. The concentrations of relatively stable chemical species, such as nitrite (NO_2^-), nitrate (NO_3^-) and hydrogen peroxide (H_2O_2) were determined (supplementary material, Figure S1D). Our dose-response studies suggested a dose-dependent effect between the energy density value of CAP and the concentration of soluble RONS in the solution (supplementary material, Figure S1D).

CAP increased the rate of *in vitro* wound closure and keratinocyte migration

Emerging evidence suggests that RONS are secondary signalling molecules, and although normal levels of RONS are essential for efficient wound closure, abnormally increased levels are detrimental [30]. We recently identified the optimal dose of CAP associated with improved rate of endothelial cell migration [8]. We have now determined the optimal dose of CAP for the key effector cells of skin repair (supplementary material, Figure S2 and Figure S3). Using two different *in vitro* models of cellular migration, we showed that low dose of CAP increased keratinocyte motility (Figure 1A-C and supplementary material Figure S2B). Low dose of CAP increased the rate of keratinocyte migration without influencing cellular viability, but high dose of CAP

compromised cellular viability (supplementary material, Figure S3A-B; $p < 0.01$, CAP high *vs* control) and reduced cellular proliferation (supplementary material, Figure S3C; $p < 0.05$, CAP high *vs* control). From this point, all cells were treated with the low dose of CAP (2.15 J/cm^3).

Incubation with NO_2^-, NO_3^-, H_2O_2 and PAM had no effect on scratch wound closure *in vitro*

The scratch assay is a useful *in vitro* model of wound closure and cellular migration [31]. Having established that the low dose of CAP improves the rate of *in vitro* scratch wound closure in keratinocytes (supplementary material, Figure S2B) and human foreskin fibroblasts (HFF) (data not shown), we next examined whether the low dose of CAP may influence cellular migration in primary dermal fibroblasts. Indeed, scratch wounds closed significantly faster under CAP (2.15 J/cm^3) treatment than under the control condition (Fig. 1B-D, $p < 0.05$ vs control). The exposure of aqueous solutions to CAP creates plasma-activated medium (PAM) that contains a broad range of RONS, including nitrite (NO_2^-), nitrate (NO_3^-) and hydrogen peroxide (H_2O_2) [27,32]. We initially hypothesized that one of these molecules could be responsible for increased cellular migration. This assumption was based on previous studies, which demonstrated that relatively low concentrations of extracellular H_2O_2 (≤ 10 μM) are associated with increased cellular proliferation and migration [18,33]. We determined the concentration of at least three molecules, including H_2O_2, known to be produced by CAP in aqueous solutions (supplementary material, Figure S1D). CAP-treated scratch wounds closed significantly faster than did helium-treated control wounds, whereas incubation with PAM and the exogenous addition of NO_2^-, NO_3^- and H_2O_2 had no effect on *in vitro* wound closure (Fig. 1C,D; $p < 0.05$; CAP *vs* control).

CAP activated SMAD-dependent TGF-β1 signalling pathways

In an effort to explain enhanced fibroblast migration, we next hypothesised that CAP treatment is associated with increased collagen production *in vitro*. Collagens, which constitute the main structural element of the skin's ECM, are transcribed and secreted by fibroblasts [11]. Collagen-rich matrix enhances cellular migration by providing scaffolding for the epidermal and dermal cells to crawl along. Indeed, primary dermal fibroblasts treated with CAP produced higher levels of both intracellular (Fig. 2B) and secreted collagen (Fig. 2C and D). This finding raises the striking possibility that fibroblasts may migrate more easily on collagen-rich substrate, which may explain increased scratch wound closure in CAP-treated fibroblasts (Fig. 1D). To identify mechanisms that facilitated increased collagen I production in CAP-treated fibroblasts, protein activation studies involving canonical TGF-β cascades were performed *in vitro*. Confocal microscopy studies showed that CAP caused the translocation of pSMAD2 from the cytoplasm into the nucleus (Fig. 2A) and robustly upregulated intracellular pSMAD2 in primary dermal fibroblasts (Fig. 2B and supplementary material, Figure S4).

CAP increased the rate of cellular outgrowth and migration *ex vivo*

The *in vitro* assays summarised in Fig. 1 and Fig. 2 were performed using human epidermal and dermal cells, whereas the *ex vivo* assay described in supplementary material, Figure S5 was based on the mouse skin. For consistency, we used mouse skin tissue in the *ex vivo* assay because our *in vivo* model involved mice. In the *ex vivo* explant assay, mouse skin was cultured over 8 days. On day 2 post-culture, a cellular halo composed of migrating cells appeared around the explants. Compared with helium-treated controls, skin explants treated with CAP (2.15 J/cm^3) displayed a significant increase in cellular migration (supplementary material, Figure S5A,B).

Enhanced wound closure in response to CAP *in vivo*

The effect of treatment with CAP was tested in a murine model of full-thickness burn wounds reconstructed with allogeneic skin grafts. Several temperature and time combinations were tested to establish an experimental protocol with reproducible outcomes (supplementary material, Figure S6). Histological analysis of the epidermis and dermis was performed to identify known indicators of tissue injury, including blocked vessels, infiltration of inflammatory cells, and presence of adipose and muscle layers. The exposure of skin to 80 ºC for 20 seconds consistently produced full-thickness burn wounds, which macroscopically appeared as circular wounds with white eschar and a surrounding hyperaemic zone (supplementary material, Figure S6A). When the eschar and hyperaemic zones were debrided 24 h after burn injury, the area of the resulting wound was larger than that of the initial burn. After debridement, the wounds were reconstructed with a full-thickness skin graft (Fig. 3A). Grafted wounds that received CAP treatment or helium showed no signs of transplant rejection (Fig. 3B). The histological wound gape (Fig. 3C and D; $p < 0.05$) and re-epithelialisation rate (Fig. 3D; $p < 0.01$) showed that wounds treated with CAP had significantly smaller microscopic wound sizes than did helium-treated controls.

CAP modulated the expression of DEJ components in transplanted grafts

Laminin 5 and collagen IV are major components of the DEJ [34]. To assess DEJ integrity, day 7 mouse wounds were stained with anti-laminin 5 and anti-collagen IV antibodies (Fig. 4A). Compared with control wounds, CAP-treated wounds were associated with increased laminin 5 and collagen IV density (Fig. 4B; $p < 0.01$). Fibronectin is an adhesive protein that mediates cell

attachment and provides a scaffold for fibroblast migration during wound healing [11,35]. CAP treatment showed no effect on fibronectin expression (Fig. 4B).

Treatment with low dose of CAP *in vivo* is associated with increased epidermal and dermal tissue proliferation

Epidermal and dermal cells in CAP-treated wounds expressed Ki67 (proliferation marker). Ki67 is expressed at the migrating tongue of the epidermis around the wound edge and within the dermal wound bed in CAP-treated wounds and controls (Fig. 5A). Ki67 was significantly increased in CAP-treated wounds compared to time-matched controls (Fig. 5B; $p < 0.01$). To investigate whether repeated treatment with CAP could be associated with negative effects on the cutaneous tissue, mouse wounds exposed to CAP treatment were harvested at day 7 and stained with caspase 3 (marker of apoptosis) [36]. Caspase 3 immunohistochemistry staining of day 7 mouse wounds showed that CAP treatment was not associated with apoptotic changes (Fig. 5C). While CAP-treated mouse wounds were negative for caspase 3, positive caspase 3 immunohistochemistry staining was evident in intestinal epithelium of $Atg7^{-/-}$ mice treated with tamoxifen (Fig. 5D). Positive staining for caspase 3 indicates cytotoxic damage and apoptosis, and is evident in both differentiated villi and proliferative crypts of $Atg7^{-/-}$ intestinal epithelium (Fig. 5D). Irradiated and tamoxifen-treated $Atg7^{-/-}$ mice were described elsewhere [37], and microscopic sections of the $Atg7^{-/-}$ small intestine were kindly provided by the authors of the abovementioned work. Microscopic sections of day 7 mouse wounds treated with CAP were negative for TUNEL (terminal deoxynucleotidyl transferase dUTP nick end labelling) - indicator of apoptosis and DNA fragmentation (Fig. 5E). Histological sections of CAP-treated mouse wounds exposed to DNase I

(positive control) resulted in intense staining of the nuclei (brown) of both epidermal and dermal cells (Fig. 5E).

Increased collagen I protein expression in CAP-treated wounds and skin grafts

Having demonstrated that CAP improved burn wound repair and graft integration, we next hypothesised that these effects were partly due to enhanced ECM and collagen deposition. TGF-β1 is a potent stimulator of collagen synthesis, and collagen I is an important component of the ECM [11]. CAP treatment was associated with increased mRNA levels of *Tgfbr1* in day 7 wounds (Fig. 6A; $p < 0.05$). Detection of the active form of TGF-β1 protein is limited by the lack of specific antibodies designed to differentiate between the latent and active forms of TGF-β1. Hence, an anti-pSMAD2/3 antibody was used as an indicator of the active form of TGF-β1 protein in the mouse wounds (Fig. 6B and C). Increased expression of *Tgfbr1* mRNA in CAP-treated wounds coincided with elevated levels of collagen I deposition and pSMAD2/3 expression compared with time-matched controls (Fig. 6C; $p < 0.05$ for collagen I and $p < 0.01$ for pSMAD2/3). Collagen was visualized using second harmonic generation (SHG) imaging [38] and Masson's trichrome staining (Fig. 6D and E). CAP-treated samples were associated with a higher SHG signal compared to controls (Fig. 6F and supplementary material, Figure S7). A schematic representation of pathways likely to be modulated by CAP are shown in Supplementary Material Fig. S8.

DISCUSSION

Cutaneous injuries share a common dynamic process with overlapping phases of inflammation, new tissue formation, and remodelling [39]. Each of these processes relies on proliferation and

cellular migration, which may be observed during extravasation of monocyte-derived macrophages with subsequent translocation into the wound site and migration of keratinocytes during wound re-epithelialisation [40]. We demonstrated that treatment of endothelial cells [8] and epidermal keratinocytes with low-dose plasma did not have a detrimental effect on cellular proliferation. High-dose plasma is known to activate a cascade of cellular responses leading to the arrest of DNA replication with the subsequent induction of apoptosis [41,42]. CAP-treated malignant cells are more susceptible to apoptosis than healthy cells [43]. This suggestion arose from the observation that identical CAP dose resulted in different programmed cell death responses in malignant *vs*. healthy cells [43]. Therefore, it is reasonable to hypothesise that the power is not the only determining factor, and that other parameters, such as the cell type and concentration of CAP-generated RONS, may determine the nature of biological responses induced by CAP.

It was hypothesised that direct treatment with a low dose of CAP will enhance cellular migration *in vitro* via plasma-generated RONS. RONS are either produced in plasma-activated medium or transferred from the gas phase of plasma to aqueous media solution where they dissolve, diffuse and interact with cells [27]. Although the question of how CAP-generated RONS are delivered to cells remains to be answered, our data confirms published reports [8,29,41] and suggests that exposure to direct CAP is associated with enhanced cellular migration *in vitro*. Keratinocytes treated with CAP were previously shown to express higher levels of epidermal integrins - cellular adhesion molecules known to facilitate migration and re-epithelialisation [44]. The incubation of cells with H_2O_2, NO_2^-, NO_3^- and PAM failed to enhance cellular migration, whereas CAP-treated cells that encountered a broader range of both short- and long-lived chemical species showed increased rates of cellular migration. Firstly, these results suggest the importance of the interaction between the short- and long-lived species generated by CAP. Secondly, in addition to the role of

reactive chemical species, the influence of the physical factors also produced by CAP must not be underestimated. For instance, stimulation with moderate levels of electromagnetic field (a physical factor associated with CAP) is known to enhance motility by guiding cells to migrate into the wound [45].

TGF-β1 signals via two heterodimeric transmembrane receptors, the type 1 and type 2 receptors [15]. The TGFR1-mediated phosphorylation of SMAD2 and SMAD3 leads to activation of collagen I gene transcription. To define the upstream mechanisms of CAP-induced collagen I protein synthesis, we tested the effect of pharmacological inhibitors of the TGFR1 pathway. We provided evidence that CAP upregulated collagen I synthesis *in vitro* and *in vivo* via SMAD-dependent pathway. H_2O_2, NO_2^-, NO_3^- are RONS produced by our plasma jet. Interestingly, simultaneous treatment of fibroblasts with a mixture of these soluble RONS stimulated collagen secretion in a way similar to CAP. This finding suggests that H_2O_2, NO_2^-, NO_3^- produced by CAP could be responsible for the stimulation of collagen production by fibroblasts *in vitro*. Indeed, Luo *et al.* showed that the exogenous addition of RONS such as H_2O_2 (0 - 1000 μM) increased TGF-β1 expression in a dose-dependent manner, whereas the removal of extracellular H_2O_2 by catalase reduced TGF-β1, collagen I and collagen III protein expression in fibroblasts [46]. These results, together with our findings, highlight a role for RONS in mediating the effects of TGF-β1 and collagen. It must be pointed out that further studies are required to increase our understanding of the mechanisms related to the interaction between TGF-β1 signalling and RONS in the mediation of collagen synthesis.

Increased rate of re-epithelialisation following CAP treatment was demonstrated in a murine model of burn repair. Previous studies suggested that high doses of CAP (< 0.13 W/cm^2) can damage cutaneous tissue [47], whereas lower doses of CAP have a positive effect on wound

healing. CAP improved graft integration and viability, which coincided with the increased number of proliferating cells both in the dermis and epidermis in CAP-treated wounds compared to control wounds. Increased graft integration was probably due, in part, to the improved restoration and deposition of essential components of DEJ-BM - vital for the epidermal-dermal adherence and mechanical support of the epidermis.

In the clinical setting, the transplantation of allogeneic skin grafts is associated with an immune response leading to rejection of the graft; hence, allografts are used as short-term biological dressings [1,7], whereas long-term allograft survival warrants an immunosuppressive therapy [35]. No signs of graft rejection were evident during the course of this study despite the donor and recipient mice being different individuals of the same species, but not syngeneic. The absence of rejection and the evidence of graft integration could be due to two reasons. First, the time at which the experiment was terminated was less than 3 weeks, whereas in the clinical setting (provided that no immunosuppressive therapy was implemented), rejection occurs 3 weeks after the initial use of allografts [1]. Second, the donor and recipient animals were derived from the same inbred strain, making them genetically similar (if not identical), and hence immunologically compatible. This most likely prevented the immune rejection response.

Significant improvement in burn repair and skin graft integration in wounds treated with CAP was possibly due to the enhanced formation of the ECM. The increased levels of *Tgfbr1* mRNA, activation of SMAD2 and upregulation of collagen I in CAP-treated mouse wounds pointed to the involvement of TGF-β1 signalling pathways. Collagen is the most abundant fibrous protein within the ECM [39], and the production of type I collagen is crucial for cellular migration, matrix maturation and skin elasticity [1]. Previous studies of CAP-treated mouse wounds measured skin stiffness (or measurement of resistance when a force is exerted on elastic skin) and showed that

CAP was associated with increased wound stiffness in the proliferative phase of wound repair [48]. Our study, together with previous reports [28,48], indicates that collagen I synthesis is enhanced in CAP-treated wounds, which strengthens the wound and may be beneficial during the early phase of wound healing. We recently demonstrated that CAP treatment is associated with enhanced formation of functional blood capillaries *in vivo* [8]. Given that collagen I is known to positively affect endothelial cell survival, angiogenesis and vessel lumen formation, and that embryonic lethal mutation in collagen I gene causes rupture of blood vessels [49], it is reasonable to hypothesise that increased angiogenesis in CAP-treated mouse wounds was further facilitated by collagen-rich ECM.

In summary, CAP treatment was associated with enhanced cutaneous wound repair and graft integration. Our studies demonstrate that CAP is a positive regulator of at least two important responses to cutaneous wounding, angiogenesis, and ECM formation.

CONFLICT OF INTEREST

The authors confirm that there are no known conflicts of interest associated with this publication and there has been no significant financial support for this work that could have influenced its outcome.

ACKNOWLEDGEMENTS: This work was supported by La Direction Générale de L'Armement, l'Agence de l'Innovation de Défense and École Polytechnique. We thank Mr Benoit Peuteman and Ms Charlotte Auriau from INSERM Lavoisier (SEIVIL) US 33, Hôpital Paul Brousse, Villejuif for technical assistance and scientific discussions. The authors thank Dr Béatrice

Romagnolo and Romain Sanson of INSERM U1016, Institut Cochin, Paris, France for providing with samples of radiotherapy and chemotherapy-treated Atg7 knockout mouse intestinal tissue.

AUTHOR CONTRIBUTIONS: NF, J-JL and AR conceived and designed the experiments, CD and NF carried out all experiments, acquired, analysed and interpreted data. MF and RO prepared samples for histological analysis and carried out all the experiments involving immunohistochemistry. GU and SB contributed substantially to analysis, interpretation of data and critical revision of the manuscript for its important intellectual content. NF wrote the manuscript. All authors contributed to manuscript preparation and approved the final submitted versions.

REFERENCES

1. Sun BK, Siprashvili Z, Khavari PA. Advances in skin grafting and treatment of cutaneous wounds. *Science* 2014; **346**: 941-945.
2. Ramsey ML, Patel BC. Full Thickness Skin Grafts. In: StatPearls. (ed)^(eds): Treasure Island (FL), 2019.
3. Chandrasegaram MD, Harvey J. Full-thickness vs split-skin grafting in pediatric hand burns--a 10-year review of 174 cases. *J Burn Care Res* 2009; **30**: 867-871.
4. Brusselaers N, Pirayesh A, Hoeksema H, *et al.* Skin replacement in burn wounds. *J Trauma* 2010; **68**: 490-501.
5. Greenhalgh DG. Management of Burns. *N Engl J Med* 2019; **380**: 2349-2359.
6. Adams DC, Ramsey ML. Grafts in dermatologic surgery: review and update on full- and split-thickness skin grafts, free cartilage grafts, and composite grafts. *Dermatol Surg* 2005; **31**: 1055-1067.
7. Finnerty CC, Jeschke MG, Branski LK, *et al.* Hypertrophic scarring: the greatest unmet challenge after burn injury. *Lancet* 2016; **388**: 1427-1436.
8. Duchesne C, Banzet S, Lataillade JJ, *et al.* Cold atmospheric plasma modulates endothelial nitric oxide synthase signalling and enhances burn wound neovascularisation. *J Pathol* 2019.
9. Dekoninck S, Blanpain C. Stem cell dynamics, migration and plasticity during wound healing. *Nat Cell Biol* 2019; **21**: 18-24.
10. Fisher G, Rittie L. Restoration of the basement membrane after wounding: a hallmark of young human skin altered with aging. *J Cell Commun Signal* 2018; **12**: 401-411.

11. Frantz C, Stewart KM, Weaver VM. The extracellular matrix at a glance. *Journal of cell science* 2010; **123**: 4195-4200.
12. Eming SA, Martin P, Tomic-Canic M. Wound repair and regeneration: mechanisms, signaling, and translation. *Sci Transl Med* 2014; **6**: 265sr266.
13. Meng XM, Nikolic-Paterson DJ, Lan HY. TGF-beta: the master regulator of fibrosis. *Nat Rev Nephrol* 2016; **12**: 325-338.
14. Wynn TA, Ramalingam TR. Mechanisms of fibrosis: therapeutic translation for fibrotic disease. *Nat Med* 2012; **18**: 1028-1040.
15. Lichtman MK, Otero-Vinas M, Falanga V. Transforming growth factor beta (TGF-beta) isoforms in wound healing and fibrosis. *Wound Repair Regen* 2016; **24**: 215-222.
16. Gan L, Zhang S, Poorun D, *et al.* Medical applications of nonthermal atmospheric pressure plasma in dermatology. *J Dtsch Dermatol Ges* 2018; **16**: 7-13.
17. Del Rosso JQ, Kircik LH. Spotlight on the Use of Nitric Oxide in Dermatology: What Is It? What Does It Do? Can It Become an Important Addition to the Therapeutic Armamentarium for Skin Disease? *J Drugs Dermatol* 2017; **16**: s4-s10.
18. Niethammer P, Grabher C, Look AT, *et al.* A tissue-scale gradient of hydrogen peroxide mediates rapid wound detection in zebrafish. *Nature* 2009; **459**: 996-999.
19. Isbary G, Morfill G, Schmidt HU, *et al.* A first prospective randomized controlled trial to decrease bacterial load using cold atmospheric argon plasma on chronic wounds in patients. *Br J Dermatol* 2010; **163**: 78-82.
20. Isbary G, Heinlin J, Shimizu T, *et al.* Successful and safe use of 2 min cold atmospheric argon plasma in chronic wounds: results of a randomized controlled trial. *Br J Dermatol* 2012; **167**: 404-410.
21. Rutkowski R, Daeschlein G, von Woedtke T, *et al.* Long-term Risk Assessment for Medical Application of Cold Atmospheric Pressure Plasma. *Diagnostics (Basel)* 2020; **10**.
22. Grada A, Mervis J, Falanga V. Research Techniques Made Simple: Animal Models of Wound Healing. *J Invest Dermatol* 2018; **138**: 2095-2105 e2091.
23. Ruifrok AC, Johnston DA. Quantification of histochemical staining by color deconvolution. *Anal Quant Cytol Histol* 2001; **23**: 291-299.
24. Ruzehaji N, Frantz C, Ponsoye M, *et al.* Pan PPAR agonist IVA337 is effective in prevention and treatment of experimental skin fibrosis. *Ann Rheum Dis* 2016; **75**: 2175-2183.
25. Adams DH, Ruzehaji N, Strudwick XL, *et al.* Attenuation of Flightless I, an actin-remodelling protein, improves burn injury repair via modulation of transforming growth factor (TGF)-beta1 and TGF-beta3. *Br J Dermatol* 2009; **161**: 326-336.
26. Ruzehaji N, Kopecki Z, Melville E, *et al.* Attenuation of flightless I improves wound healing and enhances angiogenesis in a murine model of type 1 diabetes. *Diabetologia* 2014; **57**: 402-412.
27. Yan D, Sherman JH, Keidar M. Cold atmospheric plasma, a novel promising anti-cancer treatment modality. *Oncotarget* 2017; **8**: 15977-15995.
28. Arndt S, Unger P, Wacker E, *et al.* Cold atmospheric plasma (CAP) changes gene expression of key molecules of the wound healing machinery and improves wound healing in vitro and in vivo. *PLoS One* 2013; **8**: e79325.
29. Arndt S, Unger P, Berneburg M, *et al.* Cold atmospheric plasma (CAP) activates angiogenesis-related molecules in skin keratinocytes, fibroblasts and endothelial cells and

improves wound angiogenesis in an autocrine and paracrine mode. *J Dermatol Sci* 2018; **89**: 181-190.
30. Dunnill C, Patton T, Brennan J, *et al.* Reactive oxygen species (ROS) and wound healing: the functional role of ROS and emerging ROS-modulating technologies for augmentation of the healing process. *Int Wound J* 2017; **14**: 89-96.
31. Liang CC, Park AY, Guan JL. In vitro scratch assay: a convenient and inexpensive method for analysis of cell migration in vitro. *Nat Protoc* 2007; **2**: 329-333.
32. Yan D, Nourmohammadi N, Bian K, *et al.* Stabilizing the cold plasma-stimulated medium by regulating medium's composition. *Sci Rep* 2016; **6**: 26016.
33. Stone JR, Yang S. Hydrogen peroxide: a signaling messenger. *Antioxid Redox Signal* 2006; **8**: 243-270.
34. Goletz S, Zillikens D, Schmidt E. Structural proteins of the dermal-epidermal junction targeted by autoantibodies in pemphigoid diseases. *Experimental dermatology* 2017; **26**: 1154-1162.
35. Forbes SJ, Rosenthal N. Preparing the ground for tissue regeneration: from mechanism to therapy. *Nat Med* 2014; **20**: 857-869.
36. Miller JD, Baron ED, Scull H, *et al.* Photodynamic therapy with the phthalocyanine photosensitizer Pc 4: the case experience with preclinical mechanistic and early clinical-translational studies. *Toxicol Appl Pharmacol* 2007; **224**: 290-299.
37. Trentesaux C, Fraudeau M, Pitasi CL, *et al.* Essential role for autophagy protein ATG7 in the maintenance of intestinal stem cell integrity. *Proc Natl Acad Sci U S A* 2020; **117**: 11136-11146.
38. Guilbert T, Odin C, Le Grand Y, *et al.* A robust collagen scoring method for human liver fibrosis by second harmonic microscopy. *Opt Express* 2010; **18**: 25794-25807.
39. Eming SA, Wynn TA, Martin P. Inflammation and metabolism in tissue repair and regeneration. *Science* 2017; **356**: 1026-1030.
40. Schafer M, Werner S. Cancer as an overhealing wound: an old hypothesis revisited. *Nat Rev Mol Cell Biol* 2008; **9**: 628-638.
41. Miller V, Lin A, Kako F, *et al.* Microsecond-pulsed dielectric barrier discharge plasma stimulation of tissue macrophages for treatment of peripheral vascular disease. *Phys Plasmas* 2015; **22**: 122005.
42. Kalghatgi S, Kelly CM, Cerchar E, *et al.* Effects of non-thermal plasma on mammalian cells. *PLoS One* 2011; **6**: e16270.
43. Bauer G, Sersenova D, Graves DB, *et al.* Cold Atmospheric Plasma and Plasma-Activated Medium Trigger RONS-Based Tumor Cell Apoptosis. *Sci Rep* 2019; **9**: 14210.
44. Haertel B, Strassenburg S, Oehmigen K, *et al.* Differential influence of components resulting from atmospheric-pressure plasma on integrin expression of human HaCaT keratinocytes. *BioMed research international* 2013; **2013**: 761451.
45. Zhao M, Song B, Pu J, *et al.* Electrical signals control wound healing through phosphatidylinositol-3-OH kinase-gamma and PTEN. *Nature* 2006; **442**: 457-460.
46. Luo J, Liu X, Liu J, *et al.* Activation of TGF-beta1 by AQP3-Mediated H2O2 Transport into Fibroblasts of a Bleomycin-Induced Mouse Model of Scleroderma. *J Invest Dermatol* 2016; **136**: 2372-2379.
47. Wu AS, Kalghatgi S, Dobrynin D, *et al.* Porcine intact and wounded skin responses to atmospheric nonthermal plasma. *J Surg Res* 2013; **179**: e1-e12.

48. Chatraie M, Torkaman G, Khani M, *et al.* In vivo study of non-invasive effects of non-thermal plasma in pressure ulcer treatment. *Sci Rep* 2018; **8**: 5621.
49. Lohler J, Timpl R, Jaenisch R. Embryonic lethal mutation in mouse collagen I gene causes rupture of blood vessels and is associated with erythropoietic and mesenchymal cell death. *Cell* 1984; **38**: 597-607.

*50. Alexaline MM, Trouillas M, Nivet M, et al. Bioengineering a human plasma-based epidermal substitute with efficient grafting capacity and high content in clonogenic cells. Stem Cells Transl Med 2015; 4: 643-654.

*51. Gailhouste L, Le Grand Y, Odin C, et al. Fibrillar collagen scoring by second harmonic microscopy: a new tool in the assessment of liver fibrosis. Journal of hepatology 2010; 52: 398-406.

*52. Ruzehaji N, Avouac J, Elhai M, et al. Combined effect of genetic background and gender in a mouse model of bleomycin-induced skin fibrosis. Arthritis research & therapy 2015; 17: 145.

*53. Chen X, Nadiarynkh O, Plotnikov S, et al. Second harmonic generation microscopy for quantitative analysis of collagen fibrillar structure. Nature protocols 2012; 7: 654-669.

*54. Schmittgen TD, Zakrajsek BA, Mills AG, et al. Quantitative reverse transcription-polymerase chain reaction to study mRNA decay: comparison of endpoint and real-time methods. Anal Biochem 2000; 285: 194-204.

*Cited only in supplementary material

FIGURE LEGENDS

Figure 1. The effect of exogenous addition of NO_2^-, NO_3^-, H_2O_2 and plasma-activated medium (PAM) on keratinocyte and fibroblast migration. (A) Experimental set up. Scratch wounds were made on confluent keratinocyte and fibroblast monolayers and treated with either (i) CAP (2.15 J/cm^3), (ii) plasma-activated medium (PAM), (iii) helium (placebo control), (iv) NO_2^- at 1.5 µM, (v) NO_3^- at 0.5 µM, (vi) H_2O_2 at 10 µM or (vii) NO_2^- + NO_3^- + H_2O_2 at 1.5 µM, 0.5 µM and 10 µM respectively. HaCaT keratinocytes and primary fibroblasts were allowed to migrate and rate of scratch wound closure following treatment was recorded over a 24 h period. (B) Representative calcein stained scratch wounds are shown. The rate of closure of the *in vitro* scratch

wound in (C) and (D) was quantified as a percentage of the initial wound area. The *in vitro* scratch wound healing assay was performed in triplicates. The data are expressed as the values for repeated conditions in separate wells. Results represent mean +/− s.e.m. (n = 6, *p < 0.05, Student's t-test). ***Abbreviations used in Fig. 1:*** *cold atmospheric plasma (CAP), plasma-activated medium (PAM), hydrogen peroxide (H_2O_2), nitrite (NO_2^-), nitrate (NO_3^-).* Images from Servier Medical Art (https://smart.servier.com/) were used in the creation of this diagram.

Figure 2. Cold atmospheric plasma (CAP) activated the canonical SMAD-dependent TGF-β pathway. To determine if CAP activated SMAD2 through phosphorylation, primary human dermal fibroblasts were treated with helium (control) or CAP. (A) Confocal immunofluorescence images of skin fibroblasts stained for pSMAD2 (red). Filamentous actin was counterstained with phalloidin (green). CAP induced phosphorylation of SMAD2 (n = 6). Scale bar, 25 μm. (B) Representative western blots and bar graph showing the relative levels of collagen I, SMAD2, pSMAD2 and β-tubulin in primary human skin fibroblasts treated with helium (control), CAP, hrTGF-β1 (10 ng/ml, 5 minutes, positive control) or TGFR1 inhibitor SB431542 (10 mM, 1 h). Data represent the means and s.e.m. from 6 biologically distinct samples of primary human fibroblasts isolated from the skin of 6 healthy donors (n = 6, ∗p < 0.05, Student's t-test). The western blot images were taken from the same blot but were cropped to remove the irrelevant lanes. Full-length western blots are shown in Supplementary Fig. 4. (C) Cellular monolayers of primary human dermal fibroblasts were treated with either helium (negative control), CAP, hrTGF-β1 (10 ng/ml, 5 minutes, positive control) or TGF-β1 inhibitor SB431542 (10 mM, 1 h, negative control). After 24 h conditioned medium was collected and analysed for the effect on collagen secretion using Sircol assay (n = 4, ∗p < 0.05, Student's t-test). (D) Total soluble collagen

secreted by primary human dermal fibroblasts was measured using Sircol collagen assay in conditioned medium at 24 h after treatment with: (i) helium (control), (ii) CAP, (iii) hrTGF-β1 (10 ng/ml), (iv) plasma-activated medium (PAM), (v) NO_2^- at 1.5 µM, (vi) NO_3^- at 0.5 µM, (vii) H_2O_2 at 10 µM or (viii) at 1.5 µM, 0.5 µM and 10 µM respectively (n = 4, $*p < 0.05$, Student's t-test). ***Abbreviations used in Fig. 2:*** *cold atmospheric plasma (CAP), recombinant human transforming growth factor beta1 (rhTGF-β1), phosphorylated SMAD-2 (pSMAD2), plasma-activated medium (PAM), hydrogen peroxide (H_2O_2), nitrite (NO_2^-), nitrate (NO_3^-).*

Figure 3. **Cold atmospheric plasma (CAP) treatment enhanced burn wound and skin graft healing**. (A) Experimental timeline. Burns were created on the dorsum of each mouse. Burned skin was debrided and covered by allogeneic skin graft. Wounds were treated every second day with either helium (control) or CAP (voltage = 24 kV, time = 30 seconds). (B) Representative digital images of burn wounds reconstructed with allogeneic skin grafts on day 0, 1, 3 and 7. The ruler on images is in millimeters. White arrow indicates margins of macroscopic wound gape. (C) H&E-stained sections of wounds 7 days post-burn injury. Yellow arrows indicate the margins of the microscopic/histological wound gape. Enlarged views of the boxed regions are shown in the lower panel. Note that the length of neo-epidermis (dotted line; enlarged view) is significantly increased in CAP-treated wounds compared to controls. In C the scale bar is 100 µm (upper panel; magnification of the objective lens is 10 ×) and 50 µm (lower panel; magnification of the objective lens is 20 ×). (D) Graphical representation of the wound gape. Histological dermal wound gape was determined by measuring the distance between the dermal margin of the burn wound and dermal margin of the skin graft. (E) Percentage of wound re-epithelialisation was evaluated by measuring the length of neoepidermis at day 7 post-burn injury and expressed as a percentage of

the whole wound length. CAP treatment was associated with enhanced wound closure. Results represent mean +/− s.e.m. (n = 6 mice in control group; n = 9 mice in CAP group, $*p < 0.05$; Student's t-test). ***Abbreviation used in Fig. 3:*** *cold atmospheric plasma (CAP), Day 0 (D 0).*

Figure 4. Cold atmospheric plasma (CAP) is associated with enhanced graft integration at the burn wound site. To assess the degree of skin graft integration markers of dermal-epidermal junction (DEJ) were used. (A) Representative immunohistochemistry images of day 7 wounds stained with anti-laminin 5 and anti-collagen IV (major components of DEJ) antibodies. Fibronectin is an important component of extracellular matrix. CAP had no effect on fibronectin expression in CAP-treated wounds compared to controls. Scale bar = 50 μm in all images with the exception of Col IV. Scale bar in Col IV = 25 μm (B) Quantitative microdensitometric evaluation of laminin-5, collagen IV, and fibronectin in day 7 wounds treated with helium (control) and CAP. CAP treatment is associated with increased laminin 5 and collagen IV immunohistochemistry staining compared to control. Immunohistochemistry analysis was performed based on six fields of microscopic view of six helium (control) and nine CAP-treated wounds. Results represent mean +/− s.e.m. (n = 6 in control, n = 9 in CAP; $**p < 0.01$, Mann–Whitney U test). ***Abbreviation used in figure 4:*** *cold atmospheric plasma (CAP).*

Figure 5. Cold atmospheric plasma (CAP) is associated with increased cellular proliferation at the burn wound site. (A) Representative immunohistochemistry images of day 7 wounds stained with Ki-67 antibodies. Note that basal keratinocytes and dermal cells closest to the wound edge, notably in CAP-treated wounds, are positive for Ki67 and thus proliferating (indicated with black arrows). (B) Quantitative microdensitometric evaluation of Ki67 in day 7 wounds treated

with helium (control) and CAP. CAP treatment is associated with increased Ki67 expression compared to control. Immunohistochemistry analysis was performed based on six fields of microscopic view of six helium (control) and nine CAP-treated wounds. Formalin-fixed and paraffin-embedded day 7 mouse wounds and skin grafts were stained with Caspase 3 (marker of apoptosis). (C) Representative immunohistochemistry images of days 7 wounds treated with either helium (control) or CAP and stained with anti-caspase 3 antibodies. No activation of Caspase 3 was evident (n = 6 in control, n = 6 in CAP). (D) Representative caspase 3 staining of tamoxifen-treated $Atg7^{-/-}$ mouse intestinal epithelium (positive phenotype for caspase 3). Caspase 3-positive cells are evident in $Atg7^{-/-}$ intestinal epithelium, particularly at the lower part of intestinal villi and the crypt (n = 6). Scale bar is 50 µm. Scale bar of the micrograph with a higher magnification in D (right) is 20 µm. (E) Representative TUNEL staining of day 7 mouse wounds treated with helium (control), CAP and DNase I (1 µg/µl). Methyl green was used as a nuclear counterstain (n = 6 in control, n = 6 in CAP and n = 6 in DNase). ***Abbreviation used in figure 5:*** *cold atmospheric plasma (CAP), TUNEL (terminal deoxynucleotidyl transferase dUTP nick end labeling), deoxyribonuclease I (DNase I).*

Figure 6. Increased expression of downstream effectors of TGF-β1 signalling in CAP-treated wounds. To determine if CAP influenced *Tgfbr1* mRNA levels, day 7 wounds were excised and homogenized. RNA was isolated and examined by real-time quantitative PCR. (A) Differences were calculated using the Ct and comparative Ct methods for relative quantification. Results were expressed in arbitrary units and normalised with *Hprt1* gene. (A) The results represent mean +/− s.e.m. of triplicate determinations from four control and four CAP-treated wounds (n = 4 in control group and n = 4 in CAP-treated group; *$p < 0.05$, Student's t-test). To determine the effect of CAP

on collagen I and SMAD2/3 (downstream effectors of TGF-β1) expression in burn wounds, day 7 wounds were stained with anti-pSMAD2/3 and anti-collagen I antibodies. (B) Representative images of alkaline phosphatase-based immunohistochemistry of day 7 mouse wounds stained for collagen I, pSMAD2/3 and control for immunohistochemistry (no primary antibody). Scale bar, 25 μm. (C) Quantitative microdensitometric evaluation of immunohistochemical detection of collagen I and pSMAD2/3 in day 7 mouse wounds. Immunohistochemistry analysis was performed based on six fields of microscopic view of six control and nine CAP-treated wounds. Results represent mean +/− s.e.m. (n = 6 in control, n = 9 in CAP; *p < 0.05; **p < 0.01, Mann–Whitney U test). (D) Representative TPEF/SHG montage scans of control and CAP-treated day 7 mouse wounds. Simultaneous two-photon excited fluorescence signal (TPEF)/second harmonic generation (SHG) acquisitions were made using circular polarization of the laser beam. TPEF (green) and SHG (purple) images were pseudocoloured and overlaid. Scale bar, 1 mm. (E) Representative images of Masson's trichrome of day 7 mouse wounds. Note intense blue colour evident in CAP-treated wounds stained with Masson's trichrome staining. Scale bar, 25 μm. (F) Quantitative analysis of SHG signal in histological sections of mouse skin. Results represent mean +/− s.e.m. (n = 6 in control, n = 9 in CAP; *p < 0.05 Mann–Whitney U test). ***Abbreviations used in Fig. 6****: cold atmospheric plasma (CAP), ribonucleic acid (RNA), antibody (Ab).*